

THE MOSDEF SURVEY: MEASUREMENTS OF BALMER DECREMENTS AND THE DUST ATTENUATION CURVE AT REDSHIFTS $z \sim 1.4 - 2.6^*$

NAVEEN A. REDDY^{1,5}, MARISKA KRIEK², ALICE E. SHAPLEY³, WILLIAM R. FREEMAN¹, BRIAN SIANA¹, ALISON L. COIL⁴,
BAHRAM MOBASHER¹, SEDONA H. PRICE², RYAN L. SANDERS³, & IRENE SHIVAEI¹

ABSTRACT

We present results on the dust attenuation curve of $z \sim 2$ galaxies using early observations from the MOSFIRE Deep Evolution Field (MOSDEF) survey. Our sample consists of 224 star-forming galaxies with nebular spectroscopic redshifts in the range $z_{\text{spec}} = 1.36 - 2.59$ and high S/N measurements of, or upper limits on, the $H\alpha$ and $H\beta$ emission lines obtained with the MOSFIRE spectrograph on the Keck I telescope. Using deep multi-wavelength photometry, we construct composite spectral energy distributions (SEDs) of galaxies in bins of specific star-formation rate (SFR/M^*) and Balmer optical depth. These composites are used to directly constrain the shape and normalization of the dust attenuation curve over the full wavelength range from the UV through near-IR for typical star-forming galaxies at high redshift ($z \gtrsim 1.4$). Our results imply an attenuation curve that is very similar in shape and normalization to the SMC extinction curve at wavelengths $\lambda \gtrsim 2500 \text{ \AA}$. At shorter wavelengths, the shape of the curve is identical to that of the Calzetti et al. (2000) starburst attenuation relation, but with a lower normalization (R_V), implying less attenuation at a fixed wavelength for a given SED shape. Hence, the new attenuation curve results in SFRs that are $\approx 20\%$ lower, and stellar masses that are $\Delta \log(M^*/M_\odot) \approx 0.16$ dex lower, than those obtained with the starburst attenuation curve. We find marginal evidence for excess absorption at 2175 \AA . Moreover, we find that the difference in the reddening—and the total attenuation—of the ionized gas and stellar continuum correlates strongly with SFR, such that for dust-corrected SFRs $\gtrsim 20 M_\odot \text{ yr}^{-1}$, assuming a Chabrier (2003) IMF, the nebular emission lines suffer an increasing degree of obscuration relative to the continuum. A simple model that can account for these trends is one in which the UV through optical stellar continuum is dominated by a population of less reddened stars, while the nebular line and bolometric luminosities become increasingly dominated by dustier stellar populations for galaxies with large SFRs, as a result of the increased dust enrichment that accompanies such galaxies. Consequently, UV- and SED-based SFRs may underestimate the total SFR at even modest levels of $\approx 20 M_\odot \text{ yr}^{-1}$.

遠方銀河のダスト減光曲線はどうなっているか？

- MOSFIRE MOSDEF survey, $H\alpha/H\beta$ measurement + 多色測光
- $z \sim 2$ (1.36–2.59) star-forming galaxies 224天体
- $0.7''$ slit, $R \sim 3500$, 1hr ($z \sim 1.5$), 2hr ($z \sim 2.3$)

Fig.16: 電離ガス (輝線) と星 (連続光) に対する減光の違い

- $E(B-V)_{\text{star}}$: continuum spectra の SED fitting から。
- $E(B-V)_{\text{gas}}$: $H\alpha/H\beta$ から。
- sSFRが大きいほど、ガスが減光される傾向。

Fig.19: 星形成率に依存したガス・星・ダストの分布

- (i) 適度なdiffuse dustに覆われた星
 - (ii) 濃いpatchyダストに埋もれた星
- SFR大 \rightarrow 全体的にdust増、かつpatchy region増
 \rightarrow dusty line emission増

SFR面密度 (\sim patchiness) との相関を調べるのが次のステップ。

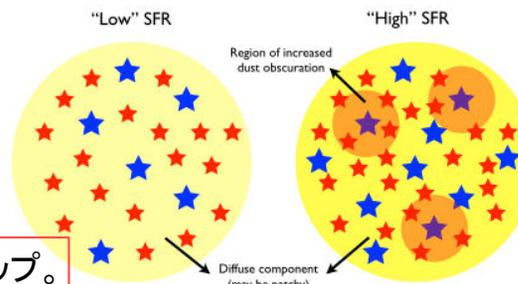


Figure 19. Illustration of a simple geometry of dust and gas that can account for the trends in the difference between ionized gas and continuum color excess, and total attenuation, versus sSFR. The yellow region denotes the diffuse dust component (that may be patchy). The red regions indicate areas of increased dustiness within the galaxy. The blue and red stars indicate high mass (ionizing) and lower mass stars, respectively. At lower SFRs ($\lesssim 20 M_\odot \text{ yr}^{-1}$), stars of all masses are uniformly obscured. As the SFR increases, the diffuse component becomes more dust-enriched (as indicated by the darker shade of yellow), while regions of more highly obscured SFR (red regions) become prominent. As the SFR increases, these more obscured regions begin to dominate the nebular line and bolometric luminosities. The diffuse component dominates the UV through optical SED at both low and high SFRs.

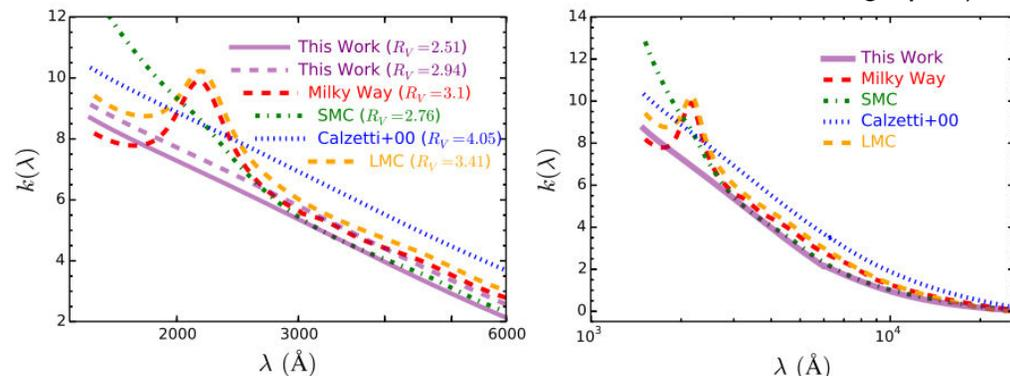


Figure 10. Left: Comparison of the MOSDEF attenuation curve assuming two different values of $R_V = 2.505$ and $R_V = 2.942$ (see text), and that of Calzetti et al. (2000) (dotted line). Also included are the local extinction curves of the Milky Way, SMC, and LMC, where the shapes and normalizations (R_V) have been taken from Gordon et al. (2003). Right: Same as left panel, where we show the MOSDEF attenuation curve assuming $R_V = 2.505$ over the full wavelength range $\lambda = 0.15 - 2.50 \mu\text{m}$.

Fig.10: MOSDEFで見積もった $z \sim 2$ 減光曲線

- $\lambda > 0.25 \mu\text{m}$ はSMCとほぼ一致。
- $\lambda < 0.25 \mu\text{m}$ はCalzetti2000と同じ傾きだが、normalization (R_V) が異なる
- 2175 \AA bumpはあるかも (完全なMOSDEFデータで要検証)。

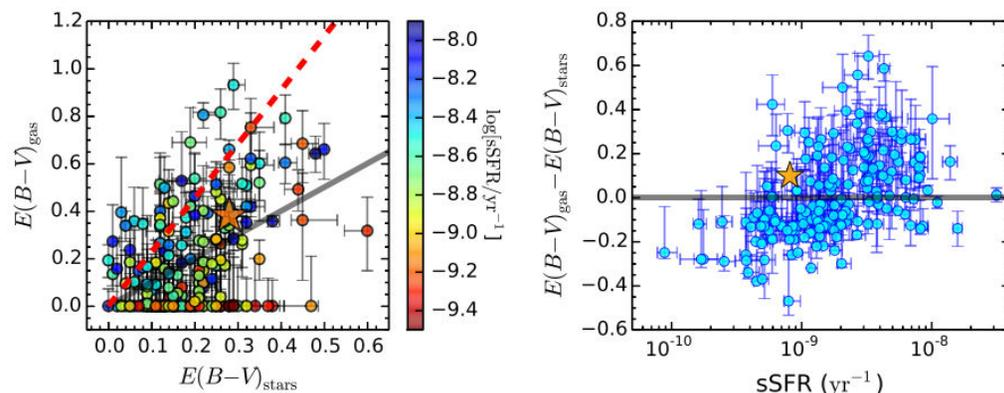


Figure 16. Left: Comparison of the color excesses derived for the stellar continuum and the ionized gas. $E(B-V)_{\text{gas}}$ is computed assuming the Cardelli et al. (1989) extinction curve, and $E(B-V)_{\text{stars}}$ is the value returned from the SED fitting when we assume the MOSDEF attenuation curve. The solid line denotes identical color excesses derived for the stellar and gas components, and the dashed line indicates the relation $E(B-V)_{\text{gas}} = E(B-V)_{\text{stars}}/0.44$ from Calzetti et al. (2000). Points are differentiated according to the sSFR. The large star denotes the average values for the $H\beta$ -undetected galaxies. Right: Difference between gas and continuum color excesses as a function of sSFR, where the solid line indicates no difference between the color excess of the nebular regions and the stellar continuum. The large star denotes the average values for the $H\beta$ -undetected galaxies.